Evidence of gate-tunable topological excitations in two-dimensional electron systems

R. Koushik,[1,*] Matthias Baenninger,[2,†] Vijay Narayan,[1,2] Subroto Mukerjee,[1] Michael Pepper,[2,‡] Ian Farrer,[2] David A. Ritchie,[2] and Arindam Ghosh[1]

[1]*Department of Physics, Indian Institute of Science, Bangalore 560012, India*

[2]*Cavendish Laboratory, University of Cambridge, J. J. Thomson Avenue, Cambridge CB3 0HE, United Kingdom*

(Received 8 October 2010; revised manuscript received 27 December 2010; published 14 February 2011)

We report experimental observations of a new mechanism of charge transport in two-dimensional electron systems (2DESs) in the presence of strong Coulomb interaction and disorder. We show that at low enough temperature the conductivity tends to zero at a nonzero carrier density, which represents the point of essential singularity in a Berezinskii-Kosterlitz-Thouless-like transition. Our experiments with many 2DESs in GaAs/AlGaAs heterostructures suggest that the charge transport at low carrier densities is due to the melting of an underlying ordered ground state through proliferation of topological defects. Independent measurement of low-frequency conductivity noise supports this scenario.

DOI: 10.1103/PhysRevB.83.085302 PACS number(s): 73.20.Qt

It has been suggested by many that strong Coulomb interaction can cause a spontaneous symmetry breaking in a two-dimensional (2D) Fermi sea of electrons, leading to a spatially charge-ordered ground state. Due to disorder these charge-density wave (CDW) states, such as Wigner crystals,[1–5] charge stripes,[6,7] etc., are pinned but offer exotic possibilities, such as metallic phases, diverging effective mass, g factors, and so on.[4] Strong many-body interaction can be induced either by lowering the carrier density n_s or by driving the system to the extreme quantum limit with a large transverse magnetic field $H_\perp$. Experimentally, however, the claims of ordered ground states have been extensive only in the latter case.[2,3,6,8–12] A difficulty is that due to pinning, the ground state is an electrical insulator, which is indistinguishable, at least in terms of dc transport, from a disordered Anderson localized ground state. Alternative experimental probes, such as activated transport,[8] broadband noise,[9,10] ac conductivity,[11] and scanning probe microscopy,[12] have yielded promising results in the high-$H_\perp$ regime, but the ground state in the low-n_s regime at low (or zero) $H_\perp$ remains less understood. Our earlier work[13] in this regime showed that the insulating phase of a disordered, yet strongly interacting 2D electron system (2DES) becomes unstable at low temperatures, showing a transition from insulating to metal-like behavior. The possibility of an interaction-induced strongly correlated phase was suggested, but the nature of such a phase, particularly the issue of ordering, remained unclear.

An aspect of ordering that has been little explored experimentally is the mechanism of "melting" to normal Fermi liquid. In 2D, infinitely long-range order does not exist at finite T. However, states with quasi-long-range order can exist, which can then undergo phase transitions into disordered (Fermi liquid) states through a Berezinskii-Kosterlitz-Thouless (BKT) type transition involving the proliferation of topological defects.[14–19] Such transitions can, in principle, be effected by varying either T or n_s (or even $H_\perp$), and the correlation length ξ in the disordered state is a nonanalytic function of the distance from the n_s-T phase boundary. Extensive theoretical work exists on topological defects in the charge-ordered phase of 2DESs, particularly in the classical Wigner crystal regime, but so far hardly any direct experimental evidence of topological defects has been observed. In this work we show that the n_s (and T) dependence of electrical conductivity σ can carry the signature of a BKT-like phase transition in strongly interacting localized 2DESs that is able to distinguish between a pinned quasiordered ground state from a disordered Anderson insulator.

The 2DESs in modulation-doped GaAs/AlGaAs heterostructures are an excellent testing ground for many-body physics because of the great control on the level of disorder. We used Si-doped GaAs/AlGaAs heterostructures (Table I), where disorder arises from the Coulomb potential of ionized Si atoms, and unintentional background doping. The devices were fabricated from GaAs/$Al_{0.33}Ga_{0.66}As$ heterostructures grown from molecular beam epitaxy, where the 2DES was formed 300 nm below the surface (see Table I). In all devices, δ (monolayer) doping of Si ($\sim 2.5 \times 10^{12}$ cm^{-2}) was implemented. The strength of the disorder is partially determined by the thickness d of the spacer layer (undoped $Al_{0.33}Ga_{0.66}As$) situated between the GaAs-AlGaAs interface and the dopant layer. The typical as-grown electron mobility was between 0.9 and 2×10^6 cm^2/V s. The wafers T546 ($d = 80$ nm) and C2367 ($d = 60$ nm) were grown in different chambers and have different background doping. For strong Coulomb interactions, it is important to achieve a low pinch-off n_s (where the conductivity goes to zero), which is difficult in macroscopic devices. This is because in macroscopic systems the inhomogeneous charge distribution constricts the electrical transport at low densities.[20,21] Mesoscopic 2DESs are more suitable since they are relatively insensitive to long-range fluctuations in the conduction band,[13,22] and hence, they form the backbone of our experiments.

The devices were patterned in the form of a microbridge with a crossed metallic surface gate [Fig. 1(a)] (Ref 13), limiting the effective area of the device to a width of $\sim 8\ \mu$m and a length of ~ 0.5–$4\ \mu$m. With decreasing n_s (negative potential on the gate), σ dropped rapidly in all devices, as illustrated in Fig. 1(c). At low T ($\lesssim 0.5$ K), small modulations on an overall smooth variation of σ were observed occasionally, which were not reproducible on thermal cycling. The carrier density where $\sigma \to 0$ decreases with increasing T [shown in Fig. 1(c) for device C2367] but increases with increasing $H_\perp$ [shown in

TABLE I. Details of devices used in our measurements showing the doping concentration n_D (10^{12} cm^{-2}), spacer thickness d (nm), as-grown mobility μ (10^6 cm^2/V s), and melting density n_{KT} at 1.5 T (10^9 cm^{-2}).

Wafer	n_D	d	μ	n_{KT}
A2407	2.5	20	1.217	7.64
A2678	2.5	40	1.8	4.38
C2367	0.7	60	1.2	10.06
T546	1.9	80	0.9	2.94

the bottom right inset of Fig. 1(c) for T546]. The pinch-off can occur at very low $n_s \lesssim 2 \times 10^9$ cm^{-2}, corresponding to an interaction parameter $r_s = 1/a_B^* \sqrt{\pi n_s} \simeq 13$, where a_B^* is the effective Bohr radius, and hence, the possibility of a CDW ground state arises naturally.

A generic signature of pinned CDW, exploited for 1D Peierls conductors[23] as well as magnetically stabilized 2D electron solids,[10] is the broadband noise (BBN) from the electric-field-induced thermally activated transitions between the metastable steady states. To explore this possibility, we have measured BBN in our mesoscopic devices at $T \approx$ 270 mK using a four-probe ac + dc technique with the ac bias fixed at $\approx 30\mu$V at an excitation frequency of 128 Hz and dc bias varied over ± 400 μV. The voltage fluctuations across the sample were measured using a lock-in amplifier whose output was subsequently digitized using a 16-bit digitizer, followed by decimation and power spectral density (PSD) calculations using Welch's method of averaged periodogram. In the insulating regime (resistivity $\gg h/e^2$), the differential resistance (dV/dI) decreases, but without any abrupt threshold, when $|V_{sd}|$ (dc voltage across the device) increases. This is illustrated for A2678 at $T = 262$ mK and $H_\perp = 0$ T in Fig. 2(a). However, when dV/dI was recorded as a function of time (over several hours) at fixed V_{sd}, we observed a random switching noise for $|V_{sd}| \sim$ 100–200 μV [see time traces in Fig. 2(b)]. The net variance of noise $\delta\sigma^2/\sigma^2$ hence shows a peak at a device-specific V_{sd} of $V_0 \approx 150 - 200$ μV. Away from this regime, the noise is largely featureless, with a power spectral density $\propto 1/f^\alpha$ [Fig. 2(c)], with the spectral exponent $\alpha \approx 1$ [Fig. 2(d)], arising from random potential fluctuations at the nearby acceptor sites. As shown in Fig. 2(e), the peak in BBN decreases rapidly with increasing n_s, and in the metallic regime, $\sigma \gg e^2/h$, it decreases below the measurement background ($\delta\sigma^2/\sigma^2 \ll 10^{-10}$). The nonmonotonicity in noise is unlikely to arise from hopping, and the absence of any slow kinetics, history dependence, or hysteresis effects in electron conductivity rules out electron glass behavior.[24] This leads to the possibility of an electrically driven depinning transition in

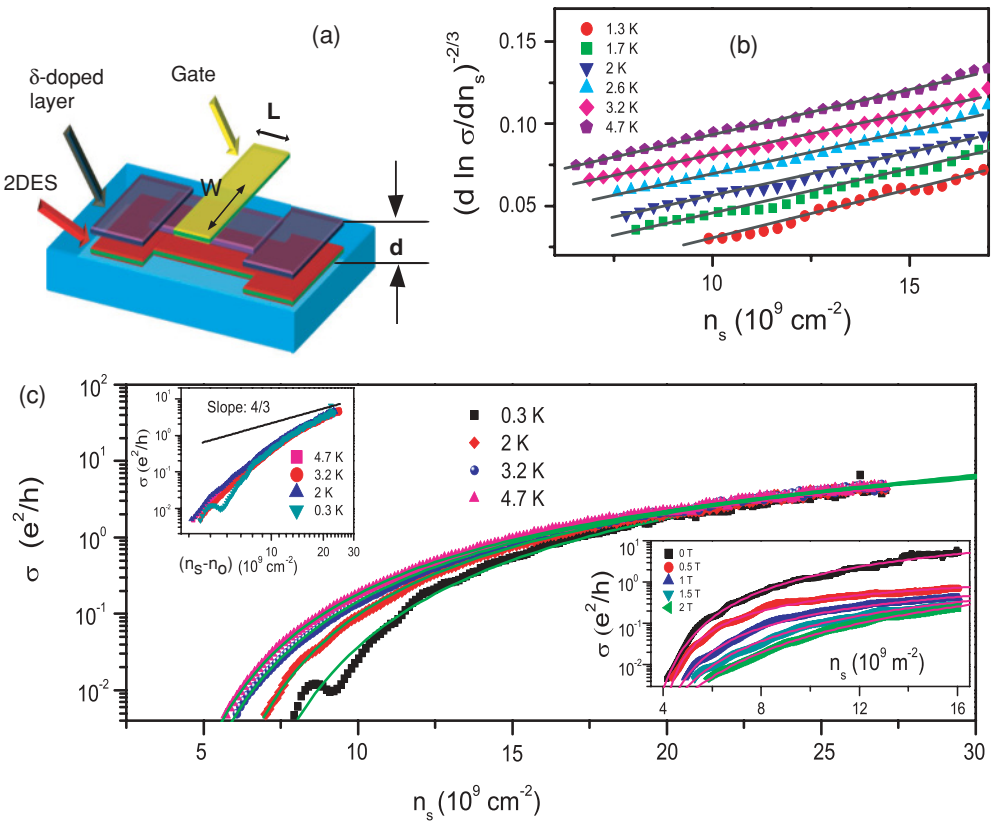

FIG. 1. (Color online) (a) Schematic of a mesoscopic device geometry showing the 2DES (red) at the heterointerface and the dopant layer (light blue). (b) Linearity of $(d \ln\sigma/dn_s)^{-2/3}$ with n_s, where the traces have been shifted vertically for clarity (device C2367). (c) Conductivity σ (device C2367) as a function of n_s at different temperatures. The solid lines are the fits for the BKT transition [see Eq. (1)]. The bottom right inset shows data and BKT fits for conductivity σ of device T546 vs n_s at different magnetic fields and $T = 262$ mK. The top left inset shows the model for percolation-based transport. The conductivity clearly shows a deviation from the power law exponent 4/3 that is expected for the case of classical percolation.

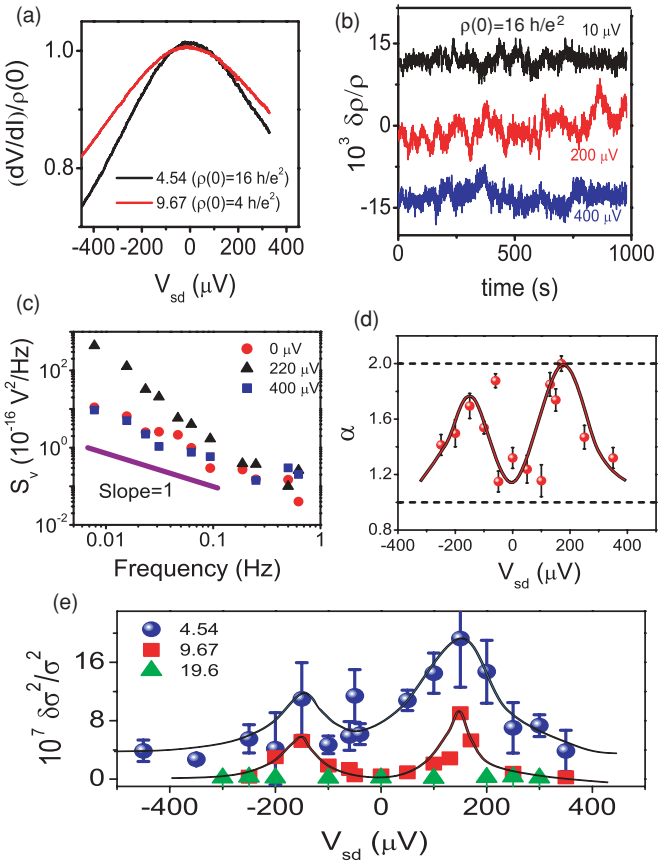

FIG. 2. (Color online) (a) Differential resistivity measurements (A2678) as a function of dc source-drain bias V_{sd} at 0.3 K and two carrier densities (10^9 cm^{-2}) corresponding to zero-bias resistivities of 4 h/e^2 and 16 h/e^2. (b) Time traces of normalized conductivity fluctuations at three different source-drain biases at $n_s = 4.54 \times 10^9$ cm^{-2}. Data show significant broadband noise at bias of $V_0 \approx 200\ \mu$V. (c) The power spectral density of conductivity noise at the three biases, showing a typical $1/f^{\alpha}$ behavior, where α is the spectral exponent ($n_s = 4.54 \times 10^9$ cm^{-2}, $T = 0.3$ K). (d) The plot of α as a function of dc bias which shows a peak magnitude of ≈ 2 around V_0. The solid line is a guide to the eye ($n_s = 4.54 \times 10^9$ cm^{-2}, $T = 0.3$ K). (e) Normalized variance $\delta\sigma^2/\sigma^2$ as a function of dc bias across the sample at different carrier densities (in units of 10^9 cm^{-2}). The solid lines are a guide to the eye ($T = 0.3$ K).

a pinned CDW ground state.[10,17] Then the bias V_0 at the noise maximum represents the depinning threshold, which depends on the quenched disorder and, hence, is only weakly dependent on n_s. The intermittent plastic flow of the CDW provides the switching noise for which α is expected to ≈ 2, as indeed observed[25] [Fig. 2(d)].

Evidence of topological defects was subsequently obtained by scrutinizing the dependence of σ on n_s. However, we first note that a classical percolation, $\sigma \sim (n_s - n_0)^{4/3}$ for $n_s > n_0$, where n_0 is the percolation threshold,[26] fails to describe the variation of σ in the localized regime. Classical percolative mechanisms can, indeed, describe conductivity at low densities, but only in macroscopic devices where charge inhomogeneities result in many "weak links" between the source and drain. As detailed in our earlier work,[22] the effect of inhomogeneity is minimal in our mesoscopic devices, and

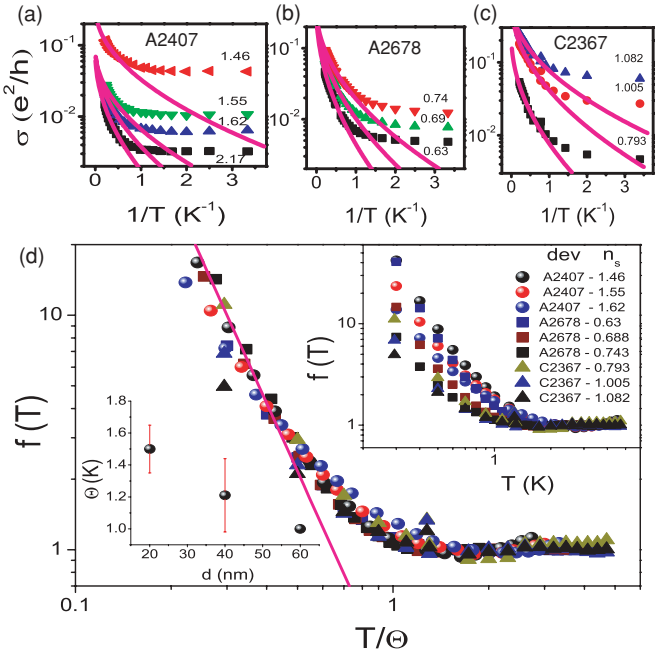

FIG. 3. (Color online) (a–c) Temperature dependence of conductivity σ in three devices of different setback distances at various densities (in units of 10^{10} cm^{-2}). The solid lines are fits at the higher temperature range ($T > 1.5$ K) for temperature-induced BKT transition [Eq. (1), $X = T$]. (d) Scaling of scattering function $f(T)$ (see text). A single parameter scaling can be observed (holding the parameter Θ for A2678 at 6.3×10^9 cm^{-2} as a reference). The line indicates an asymptotic behavior of $f(T) \approx 1/T^3$ for $T \ll \Theta$. The top right inset shows experimental $f(T)$ in various devices at different n_s (10^{10} cm^{-2}). The bottom left inset shows the scaling parameter Θ to increase with increasing disorder.

the classical percolation equation fails to describe the n_s dependence of σ [top left inset of Fig. 1(c)]. A near-saturation or even occasional metallic behavior[13] of σ at $T \lesssim 1$ K excludes variable range hopping as well [Figs. 3(a)–3(c)]. On the other hand, in a disordered CDW ground state, electrical transport can be mediated by proliferation of unbound charged topological defects. Since σ would be proportional to the number density n_{ex} ($\sim 1/\xi^2$) of such defects,[27] the BKT scaling implies

$$\sigma \propto \xi^{-2} \simeq \sigma_0 \exp\left[-\frac{A}{(X - X_{KT})^{1/2}}\right], \qquad (1)$$

where $X = n_s$ or T. When $X > X_{KT}$, where X_{KT} represents the "melting point," topological defects unbind, resulting in finite conductivity in the otherwise insulating pinned CDW state. Indeed, we find Eq. (1) describes the variation of σ as a function of n_s over several decades in all devices over T ranging from 0.3 to 4.5 K and $H_\perp$ from zero to several Tesla. (See the fits in solid line in Fig. 1(c), where σ_0, A, and n_{KT} are fit parameters.) The self-consistency of the fits can also be confirmed by the linearity of $(d \ln\sigma/dn_s)^{-2/3}$ in n_s over a factor of ~ 4 [Fig. 1(b)], where the intercept on the n_s axis gives the magnitude of n_{KT}.

To check if the analysis is physically meaningful, we constructed a melting phase diagram with n_{KT} extracted from the fits. First, we note that disorder can also stabilize

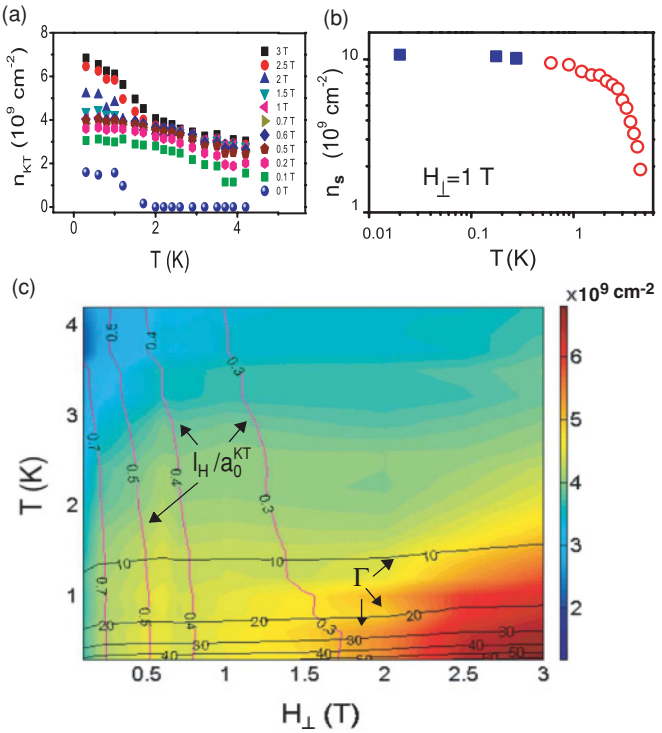

FIG. 4. (Color online) (a) Evolution of n_{KT} as a function of temperature at different magnetic fields $H_\perp$ in A2678. (b) Phase boundary of melting at $H_\perp = 1T$, showing consistency in the fits for n_{KT} and T_{KT}. Blue squares indicate T_{KT} extracted at various densities, and red circles indicate n_{KT} extracted at different temperatures. (c) Phase diagram of n_{KT} in the T-$H_\perp$ space for A2678. The magnitude of n_{KT} is indicated by the scale bar on the right. The quantum fluctuations, characterized by the normalized magnetic length l_H/a_0^{KT} (a_0^{KT} is a_0 evaluated at $n_s = n_{KT}$) and the classical melting parameter Γ (see text) are evaluated at n_{KT}, and some of the traces are shown.

a CDW state, even in the absence of $H_\perp$, by suppressing the long-wavelength fluctuations and arresting the kinetic energy of the electrons.[5] This increases the melting point (i.e., n_{KT} and T_{KT}), but excessive disorder may limit the order to a very short range or produce a glassy state. For the small $H_\perp \lesssim 2$ T employed in the present experiments, the effect of $H_\perp$ is perturbative in that it leads to additional "squeezing" of wave functions, thereby reducing the nearest-neighbor overlap and the zero-point fluctuations. Hence, in a given device, this leads to a strong enhancement of n_{KT} with $H_\perp$, as illustrated for A2678 in Fig. 4(a). Note that at $H_\perp = 0$ T, n_{KT} is nearly 1×10^9 cm^{-2} at low T and corresponds to $r_s \approx 18$, which is still much smaller than the expected r_s for Wigner crystallization in 2DESs without disorder.[1]

Fig. 4(a) illustrates that even a small $H_\perp$ can increase the melting point dramatically by quenching of quantum fluctuations of the constituent "atomic sites." It agrees with the recent suggestion that melting of a quantum electron solid needs to be addressed in terms of l_H/a_0 rather than n_s alone.[2] (Here $l_H = \sqrt{h/eH_\perp}$ and $a_0 = 1/\sqrt{n_s}$ are the magnetic length and mean electron distance, respectively.) At higher $H_\perp$ ($\gtrsim$1.5 T), a further enhancement in n_{KT} appears at low T, pointing toward a different mechanism governing the stability of the CDW. To understand this, we form a surface plot of n_{KT} in T-$H_\perp$ space in Fig. 4(c), where the traces of constant classical ($\Gamma = e^2\sqrt{n_s}/4\pi\epsilon_0\epsilon_r k_B T$) and quantum ($l_H/a_0$) melting parameters at $n_s = n_{KT}$ are shown. In the top left corner, where both thermal and quantum fluctuations are strongest, the melting occurs at small n_{KT}, while the bottom right of the plot represents maximal stability. The abrupt increase in n_{KT} for $H_\perp \gtrsim 1.5$ T occurs when $l_H/a_0^{KT} \lesssim 0.3$, possibly signifying an onset of classical electron solid as the overlap of neighboring wave functions becomes progressively smaller. The value of Γ approaches $\sim$80 in this regime ($H_\perp > 2.5$ T), which agrees closely with the estimation of Γ by Thouless for a Wigner crystal.[16]

The T dependence of σ displays a peculiar weakening below a characteristic temperature scale $\Theta \sim 1$ K [Figs. 1(c) and 3(a)–3(c)] that requires further inspection. This behavior is common to all devices, and the magnitude of Θ was found to be insensitive to changing the device length (over a factor of $\sim$8), eliminating finite size effect as the cause. The description of σ by Eq. (1) also indicates n_s to be well defined, and inhomogeneity-related models do not seem to apply here.[20,21] Assuming a quasiordered CDW state, Θ was found to be close to the phonon gap of the electron solid through the following analysis: We obtain the domain size L_0 ($\approx$430 nm) from the depinning threshold V_0 ($\sim$200 μV in BBN measurements for A2678 in Fig. 2),[10] from which the phonon gap could be calculated as $\sim\hbar c_t/k_B L_0 \approx 1.0$ K (the sound velocity $c_t \sim 4.7 \times 10^4$ m s^{-1} is taken to be that of a clean Wigner crystal) for a similar range of n_s.[28–30]

Within the BKT framework, a T-driven order $\rightarrow$ disorder phase transition would involve $\sigma(T) = f(T)\exp(-B/\sqrt{T - T_{KT}})$, where T_{KT} is the melting point and $f(T)$ is some T-dependent prefactor. The T_{KT} extracted using this formula is consistent, as shown in the combined n_S-T phase diagram in Fig 4(b). (The data were taken in a separate device with a 40-nm spacer.) The open circles in Fig 4(b) represent n_{KT} evaluated at different temperatures, and the closed squares correspond to T_{KT} evaluated at different densities. In a "Drude-like" scenario, for instance, $\sigma(T) \propto n_{ex}(T)\tau(T)$, where $f(T)$ would represent the temperature dependence of the mean scattering time $\tau(T)$. The low-T weakening of σ can then be understood from the T dependence of $f(T)$ itself. To extract this, we fitted $\sigma(T)$ by $\exp(-B/\sqrt{T - T_{KT}})$ in the range $T \gtrsim 1.5$ K [lines in Figs. 3(a)–3(c)] and subsequently divided it by the fitted trace. Consequently, $f(T)$ is approximately constant for $T \gtrsim \Theta$ but increases rapidly for $T < \Theta$ [inset Fig. 3(d)]. Intriguingly, Θ acts as the only energy scale for $f(T)$, which collapses for all samples at different n_s on a reduced T axis (Fig. 3).

Considering the Drude-like scenario and assuming $f(T)$ to represent mean scattering time $\tau(T)$ of the charge-carrying species, the T dependence of $f(T)$ can be explained by an Andreev-Lifshitz-like mechanism of defect-mediated conduction in a quantum solid.[31] For $T \gg \Theta$, $\tau \rightarrow$ const, independent of T due to extensive phonon scattering, while for $T \ll \Theta$, phonons freeze out and the scattering time increases as $\sim T^{-p}$, where $p \simeq 3$, increases rapidly to weaken the T dependence of σ. Depending on the magnitude of p and the strength of $f(T)$, this may actually cause σ to *increase* with decreasing T at low T, as has been reported recently.[13]

The key results of this paper can be summarized as follows: First, both noise and scaling of $\sigma(n_s)$ indicate a quasiordered ground state in dilute 2DESs at low T. The precise nature of ordering is not known, Wigner crystallization is a strong possibility, although it is clear that disorder plays a crucial role in stabilizing such a phase. Second, the BKT scaling provides a new framework within which the transition from strong localization to metallic conduction can be viewed as an order-disorder melting transition. This is in contrast to percolation,[26] hopping,[32] or Coulomb blockade,[33] which have been observed in many experiments over the years (mostly in larger or more disordered 2DESs). Third, the BKT transition also implies the existence and proliferation of topological defects in 2DESs in semiconductors whose number density can be tuned with a gate voltage. At low temperatures, these defects carry a charge, leading to finite electrical conductivity, even if the underlying CDW is pinned. Indeed, the absence of any threshold behavior in our dV/dI measurements indicates that the system is never a true insulator.

We acknowledge the Department of Science and Technology (DST) of India and the UK-India Education and Research Initiative (UKIERI) for funding this work.

*koushikr.in@gmail.com
†Present address: Department of Physics, Stanford University, Stanford, California 94305, USA.
‡Present address: Department of Electronic and Electrical Engineering, University College London, Torrington Place, London WC1E 7JE, United Kingdom.

[1] B. Tanatar and D. M. Ceperley, Phys. Rev. B **39**, 5005 (1989).
[2] Y. P. Chen *et al.*, Nat. Phys. **2**, 452 (2006).
[3] P. D. Ye, L. W. Engel, D. C. Tsui, R. M. Lewis, L. N. Pfeiffer, and K. West, Phys. Rev. Lett. **89**, 176802 (2002).
[4] A. Camjayi, K. Haule, V. Dobrosavljevic, and G. Kotliar, Nat. Phys. **4**, 932 (2008).
[5] A. G. Eguiluz, A. A. Maradudin, and R. J. Elliott, Phys. Rev. B **27**, 4933 (1983).
[6] G. Sambandamurthy, R. M. Lewis, H. Zhu, Y. P. Chen, L. W. Engel, D. C. Tsui, L. N. Pfeiffer, and K. W. West, Phys. Rev. Lett. **100**, 256801 (2008).
[7] A. A. Koulakov, M. M. Fogler, and B. I. Shklovskii, Phys. Rev. Lett. **76**, 499 (1996).
[8] H. W. Jiang, R. L. Willett, H. L. Stormer, D. C. Tsui, L. N. Pfeiffer, and K. W. West, Phys. Rev. Lett. **65**, 633 (1990); G. A. Csathy, H. Noh, D. C. Tsui, L. N. Pfeiffer, and K. W. West, *ibid.* **94**, 226802 (2005).
[9] V. J. Goldman, M. Santos, M. Shayegan, and J. E. Cunningham, Phys. Rev. Lett. **65**, 2189 (1990).
[10] Y. P. Li, T. Sajoto, L. W. Engel, D. C. Tsui, and M. Shayegan, Phys. Rev. Lett. **67**, 1630 (1991).
[11] Y. P. Chen, R. M. Lewis, L. W. Engel, D. C. Tsui, P. D. Ye, Z. H. Wang, L. N. Pfeiffer, and K. W. West, Phys. Rev. Lett. **93**, 206805 (2004).
[12] N. B. Zhitenev *et al.*, Nature (London) **404**, 473 (2000).
[13] M. Baenninger, A. Ghosh, M. Pepper, H. E. Beere, I. Farrer, and D. A. Ritchie, Phys. Rev. Lett. **100**, 016805 (2008).
[14] V. L. Berezenskii, Sov. Phys. JETP **34**, 610 (1972).
[15] J. M. Kosterlitz and D. J. Thouless, J. Phys. C **6**, 1181 (1973).
[16] D. J. Thouless, J. Phys. C **11**, L189 (1978).
[17] M.-C. Cha and H. A. Fertig, Phys. Rev. B **50**, 14368 (1994).
[18] B. I. Halperin and D. R. Nelson, Phys. Rev. Lett. **41**, 121 (1978); **41**, 519 (1978).
[19] A. P. Young, Phys. Rev. B **19**, 1855 (1979).
[20] V. Tripathi and M. P. Kennett, Phys. Rev. B **74**, 195334 (2006).
[21] D. Neilson and A. Hamilton, Int. J. Mod. Phys. B **22**, 4565 (2008).
[22] M. Baenninger, A. Ghosh, M. Pepper, H. E. Beere, I. Farrer, P. Atkinson, and D. A. Ritchie, Phys. Rev. B **72**, 241311(R) (2005).
[23] S. Bhattacharya, J. P. Stokes, M. O. Robbins, and R. A. Klemm, Phys. Rev. Lett. **54**, 2453 (1985).
[24] S. Kar, A. K. Raychaudhuri, A. Ghosh, H. v. Lohneysen, and G. Weiss, Phys. Rev. Lett. **91**, 216603 (2003).
[25] I. Bloom, A. C. Marley, and M. B. Weissman, Phys. Rev. Lett. **71**, 4385 (1993).
[26] S. Das Sarma, M. P. Lilly, E. H. Hwang, L. N. Pfeiffer, K. W. West, and J. L. Reno, Phys. Rev. Lett. **94**, 136401 (2005).
[27] J. G. Checkelsky, L. Li, and N. P. Ong, Phys. Rev. Lett. **100**, 206801 (2008).
[28] M. Ferconi and G. Vignale, Phys. Rev. B **48**, 2831 (1993).
[29] H. A. Fertig, Phys. Rev. B **59**, 2120 (1999).
[30] R. Chitra and T. Giamarchi, Eur. Phys. J. B **44**, 455 (2005).
[31] A. F. Andreev and I. M. Lifshitz, Sov. Phys. JETP **29**, 1107 (1969).
[32] F. W. Van Keuls, H. Mathur, H. W. Jiang, and A. J. Dahm, Phys. Rev. B **56**, 13263 (1997).
[33] A. Ghosh *et al.*, J. Phys. Condens. Matter **16**, 3623 (2004).